

Prospects for forward photon measurements at LHC

Marco van Leeuwen^{1,2,a} for the ALICE-FOCAL Collaboration

¹National Institute for Subatomic Physics Nikhef, PO Box 41882, 1009 DB Amsterdam, Netherlands

²Institute for Subatomic Physics, Utrecht University, PO Box 80000, 3508 TA Utrecht, Netherlands

Abstract. We present the opportunities to experimentally probe the gluon density at small x in nuclei to explore non-linear gluon evolution, saturation and the physics of the Color Glass Condensate by measuring photon production at forward rapidity in proton-nucleus collisions at the LHC. Performance studies for π^0 and direct photon measurements based on simulations of a Forward Calorimeter (FoCal), which is under consideration as an upgrade for the ALICE detector, are presented. Other aspects of the FoCal physics program for pp, p+Pb and Pb+Pb collisions are briefly discussed as well.

1 Introduction

The large gluon density of the proton at small fractional momentum x is expected to give rise to saturation which can be described by a non-linear evolution of the gluon Parton Distribution Functions (PDFs). This saturation is expected to set in at larger x (or larger Q^2 at the same x) in nuclei than in protons, leading to a suppression of the particle yield in p-A and d-A collisions [1–3]. In addition, multi-gluon effects are expected to become important, leading to a reduced recoil yield in di-hadron correlation measurements, since the recoil momentum is carried by multiple partons, in contrast to the more conventional $2 \rightarrow 2$ scatterings in leading order collinear QCD [4, 5].

Both the single-particle suppression and the suppression of recoil yields have been observed at forward rapidities at RHIC [6–9]. However, the observed suppression is at low p_T , which raises some doubts about the validity of the separation between long and short range physics and in particular about the expected scaling with the number of binary nucleon-nucleon collisions N_{coll} . Moreover, the forward measurements at RHIC are close to the kinematic limit, where other effects, such as energy loss and transverse momentum broadening may also affect the yields [10, 11].

Forward measurements at the LHC provide the opportunity to probe smaller x than at RHIC while also being further from the kinematic limit, thus probing deeper into the expected saturation regime. Photon measurements are of particular interest since they are directly sensitive to the gluon density at low x via the quark-gluon Compton process. Here we present the physics case and performance studies for a forward electromagnetic calorimeter (FoCal) which is being considered as a possible upgrade for the ALICE experiment at LHC.

^ae-mail: marco.van.leeuwen@nikhef.nl

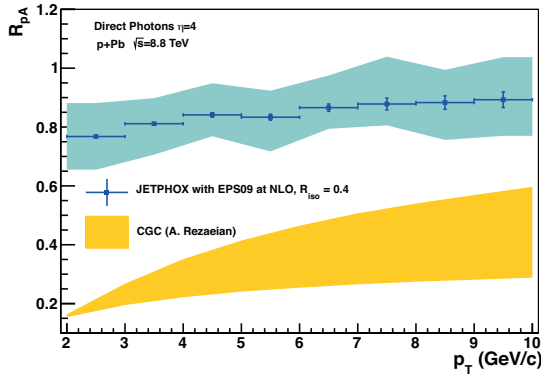


Figure 1. Expected nuclear modification factor R_{pPb} for photons at $y = 4$ at LHC. The blue area shows the result of linear evolution with the EPS09 nuclear PDFs [16] while the yellow area shows the result of a CGC calculation [17].

2 Forward photons at the LHC

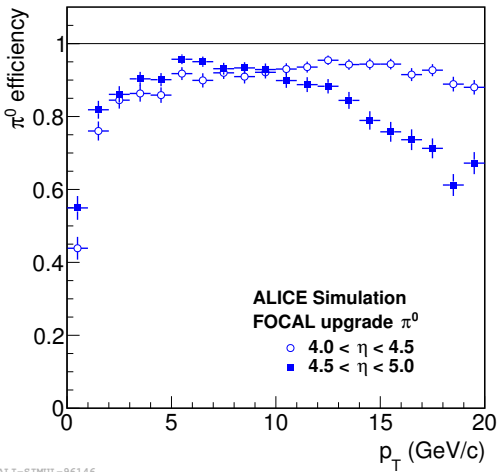
Forward particle production at rapidity 3 – 5 is being explored by LHCb and ALICE at the LHC [12, 13]. Using the back-of-the-envelope estimate that $x_2 \approx \frac{p_T}{\sqrt{s}} \exp(-y)$, it is found that at $p_T = 4$ GeV/ c and $y = 4$, one reaches $x \approx 5 \cdot 10^{-6}$ at $\sqrt{s} = 14$ TeV. Photons are an ideal probe because they are directly sensitive to the gluon density via the (dominant) quark-gluon Compton process ($qg \rightarrow q\gamma$), and the photon is directly produced in the hard process, so that the lowest x are probed at a given p_T . A more in-depth study of the x -ranges probed by direct photon and π^0 production at LHC, including Next-to-Leading Order (NLO) QCD effects, is given in [14].

Figure 1 shows the nuclear modification factor R_{pPb} for direct photons, as expected from a NLO collinear QCD calculation using JETPHOX [15], which includes nuclear effects via the EPS09 nuclear Parton Density Functions (nPDFs) [16] and a calculation using the rcBK framework for non-linear evolution [17]. The effect of gluon shadowing at small x in the nPDF-based calculation is a mild suppression $R_{pPb} \approx 0.8$, while the rcBK calculation shows a strong suppression $R_{pPb} < 0.5$ over the entire p_T range. It is expected that at even higher p_T , corresponding to larger scales Q , saturation effects are reduced and R_{pPb} in the rcBK framework approaches the nPDF results [18].

In addition to single inclusive measurements, two-particle correlation measurements can be used to probe the gluon density in the nucleus. A suppression of recoil yields associated with moderate to high- p_T π^0 and photons is expected due to multi-gluon recoil effects [5, 17, 19].

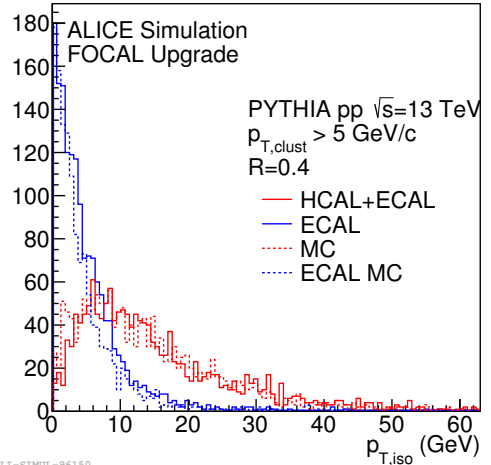
3 The FOCAL detector

The ALICE collaboration is considering to build a forward calorimeter FoCal, to measure the forward production of neutral pions and photons. This detector can be placed at about 7m from the interaction point, where it will cover about two units of pseudo-rapidity $3.3 < \eta < 5.3$. The detector would consist of a highly segmented electromagnetic calorimeter section, FoCal-E, which is capable of separating photons with a two-photon resolution of a few mm to identify decay photons, and a hadronic section FoCal-H, to improve photon-hadron separation and the measurement of isolation energy in a cone



ALI-SIMUL-96146

Figure 2. Efficiency for π^0 reconstruction in simulated events with a single π^0 including the simulated FoCal-E detector response and reconstruction algorithms in two different pseudo-rapidity ranges.



ALI-SIMUL-96150

Figure 3. Distribution of the total transverse momentum $p_{T,iso}$ in a cone with $R = 0.4$ in $\eta - \phi$ around clusters with $p_T > 5$ GeV/c from simulated p+p events. The blue curves show results using only the electromagnetic section of the FoCal, and the red curves show results with both FoCal-E and FoCal-H. The dashed curves show the results from full detector simulation and reconstruction.

around the photons, which is used to suppress contributions from decay photons and fragmentation photons.

The FoCal-E will consist of layers of Tungsten with interspersed layers of Silicon sensor material as sensitive elements. The reference design consists of 20 layers of 3.5 mm W, about 1 interaction length per layer, with 18 Low Granularity Layers (LGL) instrumented with pads of 1×1 cm² with analog readout, while 2 High Granularity Layers (HGL) with pixel sensors are used to improve the shower separation. The HGL are layer 5 and layer 10, which are around the shower maximum. In simulations, the granularity of these layers is 50 μ m, with digital readout, which are further summed into 1×1 mm² macropixels.

A prototype detector with 20 layers of full pixel read-out using Monolithic Active Pixel Sensors (MAPS) has been constructed [20, 21] and tested using beams at DESY, and CERN (PS and SPS). The results of these beams tests are very encouraging [22]. Several options for the pad technology under consideration are also being tested [23].

4 FOCAL performance

To illustrate the performance of the FoCal calorimeter, we carried out detector simulations with the FoCal in a realistic environment of the full ALICE detector using the Geant3 detector simulation package [24]. Figure 2 shows the efficiency for π^0 reconstruction as a function of transverse momentum for two forward rapidity ranges: $4 < \eta < 4.5$ and $4.5 < \eta < 5$. The efficiency here is defined as

the fraction of simulated π^0 that are fully reconstructed, by calculating the invariant mass of pairs of clusters and obtaining a value that is close to the expected mass (a window $0.07 < m_{\gamma\gamma} < 0.18 \text{ GeV}/c^2$ was used). The results were obtained with simulated events that contain a single π^0 per event for technical convenience. It was verified that the results for PYTHIA pp events with a centre-of-mass energy $\sqrt{s} = 13 \text{ TeV}$ are very similar. The reconstruction efficiency is extremely good (> 0.9) over a broad range of momenta, from a few GeV/c up to $p_T = 20 \text{ GeV}/c$ for the lower rapidity range and up to $p_T = 10 \text{ GeV}/c$ for the higher rapidity range. The high efficiency is achieved by a reconstruction algorithm that uses the high-resolution information from the HGL to split energy from the LGL into contributions from two photons. This works well for photon separations of a few mm and larger. The high efficiency will make it possible to perform precise measurements of the π^0 p_T -spectra in both pp and p+Pb collisions.

The high π^0 reconstruction efficiency is also crucial for the measurement of direct photons, since this makes it possible to tag decay photons from π^0 decay, which are the main background for direct photons.

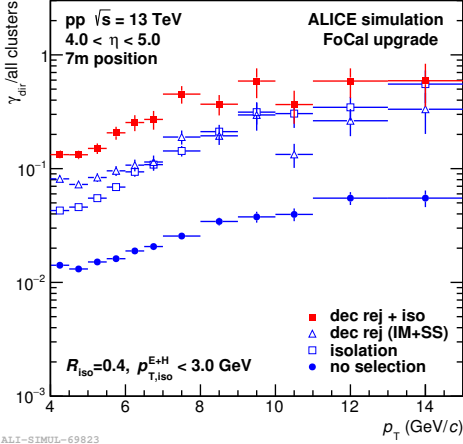
The second observable that is commonly used to identify direct photons is the isolation energy or momentum. Figure 3 shows the total transverse momentum in a cone of $R = 0.4$ in $\eta - \varphi$ around a photon candidate cluster with $p_T > 5 \text{ GeV}/c$ from simulated PYTHIA pp events with $\sqrt{s} = 13 \text{ TeV}$ with full detector response simulation. The sample of photon candidate clusters consists mostly of decay photons. The figure shows results using only the electromagnetic calorimeter (blue lines) as well as the combined FoCal-E and FoCal-H result (red lines). It can be seen in the figure that adding the hadronic calorimeter response increases the in-cone energy for decay photons significantly, which improves the effectiveness of an isolation condition to reject decay photons. We have chosen to use a cut $p_{T,\text{iso}} < 3 \text{ GeV}/c$ for further performance studies.

Figure 4 shows the signal fraction, i.e. the fraction of direct photon clusters in fully simulated pp events as a function of p_T . The solid blue circle markers show the signal fraction without background rejection, which is a few per cent at $p_T = 5 \text{ GeV}/c$ and increases to about 5% at $15 \text{ GeV}/c$. This ratio is basically given by the production cross sections of direct photons, π^0 and the decay kinematics. Using the direct rejection of decay photons with the invariant mass method or the isolation selection individually, increases the direct photon fraction by a factor 5-8; except at the lowest $p_T = 4 \text{ GeV}/c$, where the isolation cut is not very effective. The combined effect of applying both the direct decay photon rejection and the isolation cut is an improvement of the signal fraction by a factor 10, which brings the signal fraction above 0.1 over the entire range, and close to 0.5 at higher p_T . This makes it possible to measure the direct photon cross section with a relative uncertainty of about 5%.

The projected uncertainty for a direct photon measurement at forward rapidity with FOCAL is shown in Fig. 5. The dominant uncertainty in the direct photon measurement at low momentum is due the background subtraction, for which the uncertainty is given by the uncertainty on the π^0 spectrum. The uncertainties shown in the figure are obtained with a projected 5% uncertainty on the background subtraction. At high $p_T \gtrsim 10 \text{ GeV}/c$, the total systematic uncertainty is dominated by the uncertainty in the efficiency and energy scale calibration for direct photons, which is (also) assumed to be 5%, while at lower p_T the background strongly increases, leading to larger uncertainties. The dependence of the final uncertainty in that region on the γ/π^0 ratio is illustrated by showing the uncertainty estimate based on the γ/π^0 from PYTHIA (light band, larger uncertainties) and JETPHOX (dark band, smaller uncertainties).

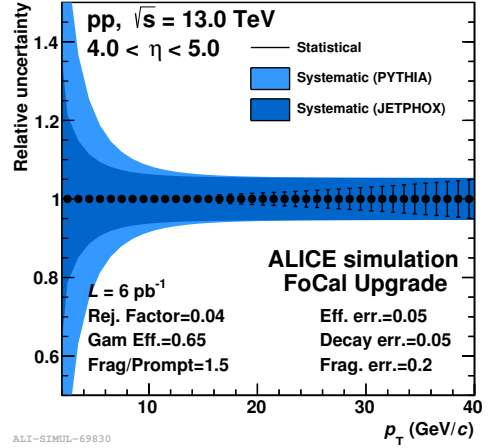
5 FoCal program in p+p and p+Pb: other observables

Besides the direct photon measurement for which the performance has been worked out in detail in the preceding section, there are a number of other measurements which are part of the FoCal



ALICE-SIMUL-69823

Figure 4. Projected γ_{dir} signal fraction in reconstructed clusters in simulated pp events with $\sqrt{s} = 13$ TeV. The solid blue points indicate the ratio without any selection cuts and the red solid points give the ratio after using both the direct rejection of decay photons based on the reconstructed invariant mass and a cut on the isolation energy $p_{T,\text{iso}} < 3\text{GeV}/c$. The open points indicated results with only the direct rejection or only the isolation cut.



ALICE-SIMUL-69830

Figure 5. Projected relative uncertainty for a direct photon measurement with FoCal in pp collisions with $\sqrt{s} = 13$ TeV, at forward rapidity $4 < \eta < 5$. Statistical and systematic uncertainties are indicated separately. The lighter band at $p_T \lesssim 10$ GeV/c indicate the projected uncertainty using the $\gamma_{\text{dir}}/\pi^0$ ratio from PYTHIA instead of JETPHOX (dark band).

program in pp and p+Pb collisions. The excellent π^0 efficiency will allow to measure both inclusive spectra and di-hadron correlations of neutral pions in the forward direction. The inclusive spectra are also sensitive to the low- x gluon density in the target, but probe larger x than photons at the same momentum. Di-hadron measurements probe the di-jet structure. Earlier measurements at RHIC have shown a broadening and depletion of the recoil yield [8, 9], which is attributed to CGC effects, where the recoil consists of multiple softer gluons instead of a single hard gluon, as expected from collinear QCD calculations [4, 5]. Exploring this phenomenon at LHC is also a key part of the FoCal physics program.

Another observable that has been suggested to explore CGC dynamics are photon-hadron correlations [17]. These will also be explored with FoCal, but the precision may be limited due to the large background of decay photons.

Finally, we can also explore longer range correlations, i.e. the near and away-side *ridge* with correlations between charged particles at mid-rapidity and neutral pions (and photons) at forward rapidity. Such correlation measurements explore dual parton scattering in the CGC-evolution, which have a non-trivial angular distribution due to interference effects [25, 26].

6 Heavy ion program for FoCal

In heavy-ion collisions, the density of produced particles in the forward direction is much larger than in pp and p+Pb collisions. In this environment, FoCal will still be able to reconstruct neutral

pions, to measure the nuclear modification factor R_{AA} at forward rapidity and study the longitudinal evolution of the medium density in such collisions as well as the effect of the larger quark jet fraction that is expected at forward rapidity [27]. These studies are complementary to measurements of J/ψ and Υ , which are found to be suppressed at forward rapidities. An independent measurement of the medium density at forward rapidity is crucial to disentangle the various mechanisms for quarkonium suppression that are being discussed in the literature, such as energy loss [28], co-movers [29] and melting due to screening effects [30, 31]. Di-hadron correlation measurements with two π^0 s will also be explored, which will provide further insight into the time evolution of the medium density. In addition, we are also exploring the potential for direct photon measurements at forward rapidity in heavy ion collisions.

References

- [1] D. Kharzeev, E. Levin, L. McLerran, Phys. Lett. **B561**, 93 (2003), hep-ph/0210332
- [2] J.L. Albacete, N. Armesto, A. Kovner, C.A. Salgado, U.A. Wiedemann, Phys. Rev. Lett. **92**, 082001 (2004), hep-ph/0307179
- [3] D. Kharzeev, Y.V. Kovchegov, K. Tuchin, Phys. Lett. **B599**, 23 (2004), hep-ph/0405045
- [4] D. Kharzeev, E. Levin, L. McLerran, Nucl. Phys. **A748**, 627 (2005), hep-ph/0403271
- [5] J.L. Albacete, C. Marquet, Phys. Rev. Lett. **105**, 162301 (2010), [arXiv]1005.4065
- [6] I. Arsene et al. (BRAHMS), Phys. Rev. Lett. **93**, 242303 (2004), nucl-ex/0403005
- [7] J. Adams et al. (STAR), Phys. Rev. Lett. **97**, 152302 (2006), nucl-ex/0602011
- [8] E. Braidot (STAR), *Suppression of Forward Pion Correlations in d+Au Interactions at STAR*, in *Proceedings, 45th Rencontres de Moriond on QCD and High Energy Interactions* (2010), [arXiv]1005.2378
- [9] A. Adare et al. (PHENIX), Phys. Rev. Lett. **107**, 172301 (2011), [arXiv]1105.5112
- [10] I. Vitev, Phys. Lett. **B562**, 36 (2003), nucl-th/0302002
- [11] Z.B. Kang, I. Vitev, H. Xing, Phys. Rev. **D85**, 054024 (2012), [arXiv]1112.6021
- [12] R. Aaij et al. (LHCb), Eur. Phys. J. **C71**, 1645 (2011), [arXiv]1103.0423
- [13] B.B. Abelev et al. (ALICE), JHEP **02**, 073 (2014), [arXiv]1308.6726
- [14] I. Helenius, K.J. Eskola, H. Paukkunen, JHEP **09**, 138 (2014), [arXiv]1406.1689
- [15] P. Aurenche, M. Fontannaz, J.P. Guillet, E. Pilon, M. Werlen, Phys. Rev. **D73**, 094007 (2006), hep-ph/0602133
- [16] K.J. Eskola, H. Paukkunen, C.A. Salgado, JHEP **04**, 065 (2009), [arXiv]0902.4154
- [17] A.H. Rezaeian, Phys. Rev. **D86**, 094016 (2012), [arXiv]1209.0478
- [18] A.M. Staśto, B.W. Xiao, F. Yuan, D. Zaslavsky, Phys. Rev. **D90**, 014047 (2014), [arXiv]1405.6311
- [19] A. van Hameren, P. Kotko, K. Kutak, C. Marquet, S. Sapeta, Phys. Rev. **D89**, 094014 (2014), [arXiv]1402.5065
- [20] G. Nooren, PoS **RD11**, 026 (2011)
- [21] D. Fehlker, J. Alme, A. Van Den Brink, A.P. De Haas, G.J. Nooren, M. Reicher, D. Röhrich, M. Rossewij, K. Ullaland, S. Yang, JINST **8**, P03015 (2013)
- [22] G. Nooren, E. Rocco, PoS **RD13**, 017 (2014)
- [23] S. Muhuri, S. Mukhopadhyay, V.B. Chandratre, M. Sukhwani, S. Jena, S.A. Khan, T.K. Nayak, J. Saini, R.N. Singaraju, Nucl. Instrum. Meth. **A764**, 24 (2014), [arXiv]1407.5724
- [24] R. Brun, F. Bruyant, M. Maire, A.C. McPherson, P. Zancarini (1987)
- [25] K. Dusling, R. Venugopalan, Phys. Rev. **D87**, 094034 (2013), [arXiv]1302.7018

- [26] A. Kovner, A.H. Rezaeian, Phys. Rev. **D92**, 074045 (2015), [arXiv]1508.02412
- [27] T. Renk (2014), [arXiv]1406.6784
- [28] F. Arleo, S. Peigné, JHEP **10**, 73 (2014), [arXiv]1407.5054
- [29] E.G. Ferreira, Phys. Lett. **B731**, 57 (2014), [arXiv]1210.3209
- [30] Y.p. Liu, Z. Qu, N. Xu, P.f. Zhuang, Phys. Lett. **B678**, 72 (2009), [arXiv]0901.2757
- [31] X. Zhao, R. Rapp, Nucl. Phys. **A859**, 114 (2011), [arXiv]1102.2194